Journal of Electroceramics, 15, 5–11, 2005


# The Applicability of Sr-deficient *n*-type $SrTiO_3$ for SOFC Anodes

T. KOLODIAZHNYI[1,*] & A. PETRIC[2]

[1]*National Institute for Materials Science, Tsukuba, Ibaraki, 305-0044, Japan*

[2]*Department of Materials Science and Engineering, McMaster University, Hamilton, Ontario, Canada, L8S 4L7*

Submitted July 13, 2004; Revised July 13, 2004; Accepted February 1, 2005

**Abstract.** Here we discuss the effect of preparation conditions on structural stability and electrical properties of Sr-deficient *n*-type $SrTiO_3$. In particular, an explanation of a wide scatter of conductivity values in Y- and Nb-doped $SrTiO_3$ reported in the literature is proposed, based on the existing defect chemistry model of *n*-doped $SrTiO_3$. It was confirmed that when sintered in air, Sr-deficient $SrTiO_3$ doped with Nb and/or Y, remains single phase until the solubility limit (e.g., 30% for Nb or 4% for Y). However, when sintered at low $P_{O_2}$ the material transforms from a vacancy compensated to an electronically compensated compound with a strontium deficient second phase. Measured at 800°C in low $P_{O_2}$, the maximum conductivity of these multi-phase compounds was 340 S/cm and 100 S/cm for the Nb-doped and Y-doped sample, respectively. However, the conductivity dropped dramatically to less than 10 S/cm when samples of the same compositions were sintered in air, again measured in reducing atmosphere.

**Keywords:** $SrTiO_3$ point defects, second phase

## 1. Introduction

Although solid oxide fuel cells (SOFC) hold the promise of efficient and environmentally benign energy conversion, the high price of the SOFC systems has been the major obstacle on the way to commercialization. As a result, research and development efforts are now focused on the cost reduction of the SOFC components and fuel cell stacks [1]. One of the possible routes being actively explored is to replace the Ni-YSZ anode which is prone to sintering, coking and sulfur poisoning by an alternative metal oxide anode. The novel anode should satisfy several important requirements, i.e., it should be thermodynamically stable in anodic conditions, catalytically active, electronically and ionically conductive and chemically inert in contact with electrolyte and interconnect. It should also possess a thermal expansion coefficient (TEC) similar to that of other SOFC components.

*To whom all correspondence should be addressed. E-mail: kolodiazhnyi.taras@nims.go.jp

Recently *n*-type $SrTiO_3$ has generated considerable optimism as an alternative SOFC anode [2–6]. Several groups indicated that $SrTiO_3$-based materials possess certain advantages over the Ni-YSZ cermet anodes, namely, adequate electronic conductivity and phase stability in a wide $P_{O_2}$ range [2, 5, 7], as well as resistance to coking and sulfur poisoning [6]. However, the high temperature conductivity value of *n*-doped $SrTiO_3$ cited by different authors varies significantly. In addition, there appears to be a thermal history component to the performance of the $SrTiO_3$-based anodes [1–6].

Due to a relatively weak $E(k)$ dependence of the conduction band electron in $SrTiO_3$, its effective mass, $m^*$, significantly exceeds the free electron mass (e.g., $m^* \approx 6 - 16m_0$) [8, 9]. This leads to rather slow conduction electrons whose drift mobility, $\mu$, decreases with temperature as expected for the phonon scattering mechanism [10]:

$$\mu \approx \mu_{no}(T/K)^{-m} \tag{1}$$

where $\mu_{no}$ is parameter dependent on the dopant concentration, $K$ stands for Kelvin, $T$ is the absolute

temperature and $m$ varies between 1.5 and 2.74 depending on the dopant concentration. Hence, in order to achieve high conductivity in polycrystalline $SrTiO_3$, a fairly high concentration of donor dopants should be employed. An insulator-to-metal transition in $SrTiO_3$ was reported [11] at a free carrier concentration of $10^{17}$–$10^{18}$ $cm^{-3}$. Above this concentration, donor impurity remains completely ionized down to 1 K [12]. Metallic conductivity in $SrTiO_3$ is realized by annealing $SrTiO_3$ in a reducing atmosphere [12–14] or by partial substitution of rare earths for Sr or Nb on Ti sites [15]. At sufficiently high donor-dopant concentrations in polycrystalline $SrTiO_3$ (e.g., 20–40 at%), conductivities of 5–500 S/cm under typical SOFC anodic conditions (i.e., $T = 800 - 1000^{\circ}C$ and $P_{O_2} = 10^{-15}$–$10^{-20}$ atm) have been reported [3–5].

From the defect chemistry viewpoint, two different approaches have been realized in the preparation of doped $SrTiO_3$ for SOFC anodes. The first approach involves sintering in air of the vacancy-compensated single phase compounds such as $Sr_{1-3x/2}La_xTiO_3$ followed by *in-situ* reduction at the SOFC anodic conditions [3]. The second approach involves formulation of the composition according to the electronic compensation regime, (e.g., $Sr_{1-x}La_xTiO_3$) and sintering in air at relatively high temperatures [5]. This latter approach results in the multi-phase compounds with partial electronic compensation of donors. Both approaches produce anodic conductivity values of the order of 10 S/cm under SOFC conditions.

Starting from the pioneering work of Seuter [16], the point defect model of the acceptor- and donor-doped perovskite titanates has been under development for the last 30 years. For general features of point defect chemistry of the titanate perovskites, the recent reviews by Moos and Härdtl [17], Smyth [18] and Meyer and Waser [19] can be consulted. Progress in the theoretical understanding of point defect equilibria in acceptor- and donor-doped $SrTiO_3$ is addressed in the work of Akhtar et al. [20].

It is known that there are two different mechanisms of donor compensation in $n$-doped $SrTiO_3$ and $BaTiO_3$, namely *electronic* at low $P_{O_2}$ and *cation vacancy type* at high $P_{O_2}$ [16, 17, 21–23]. As a result, the two thermodynamically stable phases of, for example, La-doped $SrTiO_3$ are (i) conductive $Sr_{1-x}La_xTiO_3$ at low $P_{O_2}$ [12] and (ii) insulating $Sr_{1-3x/2}La_xTiO_3$ at high $P_{O_2}$ [24]. With increasing temperature, the boundary between electronic and cation vacancy compensation regions shifts towards higher $P_{O_2}$ [21, 22].

When electronically compensated $Sr_{1-x}La_xTiO_3$ is equilibrated at high $P_{O_2}$, its transformation from electronic to cation vacancy-type compensation can be expressed by the following equation:

$$Sr_{1-x}La_xTiO_3 \Rightarrow Sr_{1-3x/2}La_xTiO_3 + \frac{x}{2}SrO_{(RP/S)}, \quad (2)$$

where $SrO_{(RP/S)}$ stands for the either Ruddlesden-Popper (RP) [25] phase of the type $Sr_{n+1}Ti_nO_{3n+1}$ incorporated into the matrix phase as a crystallographic shear plane (CSP) [26] or SrO-rich (S) second phase precipitated at the surface of the matrix composition [21].

Although it has been widely accepted that at the high oxygen activity, the donor ions are compensated in $SrTiO_3$ by strontium vacancies, the central question of whether the strontium excess is accommodated by the RP phase [26, 27] or by the SrO-rich surface phase [21] remains open. Two conflicting opinions on this problem can be found in Refs [21] and [24, 27].

Slater et al. [3] prepared single-phase $Sr_{1-3x/2}La_xTiO_3$ and $Sr_{1-y/2}Nb_yTi_{1-y}O_3$ compositions with $x \leq 0.6$ and $y \leq 0.4$ sintered in air at 1440°C in which donor ions were compensated by Sr vacancies. Conductivities of 5.6–7.0 S/cm were achieved at 930°C and $P_{O_2} = 10^{-20}$–$10^{-10}$ atm. The authors [3] also reported that porous $SrTiO_3$ samples followed the $\sigma \propto [P_{O_2}]^{-1/4}$ dependence whereas the dense samples showed anomalously weak $\sigma$ *versus* $P_{O_2}$ dependence. In contrast to Slater et al., Marina et al. [5] formulated their samples assuming electronic compensation of donor ions and reported single-phase $Sr_{1-x}La_xTiO_3$ compositions with $x \leq 0.4$ sintered in air at 1650°C with a maximum conductivity of 16 S/cm at 1000°C and $P_{O_2} = 10^{-18}$ atm. Microcracking of the La-doped $SrTiO_3$ was observed for samples sintered in reducing atmosphere and subjected to high $P_{O_2}$. The authors [5] also found that "equilibrium" $\sigma$ at a given $P_{O_2}$ depends on the $P_{O_2}$ during the sintering of ceramics.

Strontium-deficient, yttrium-doped $SrTiO_3$ was a focus of previous investigation in our lab [4]. Very high conductivities of up to 82 S/cm at 800°C and $P_{O_2} = 10^{-14}$ atm were observed for $Sr_{1-3x/2}Y_xTiO_3$ with $x = 0.08$ [4]. However, one of the most controversial results reported in Refs. [4] and [6] was that $Sr_{1-3x/2}Y_xTiO_3$ and $Sr_{1-x/2}Nb_xTi_{1-x}O_3$ remain single phase up to 1400°C and oxygen partial pressure 1–$10^{-20}$ atm in disagreement with a point defect model

of *n*-doped $SrTiO_3$. In this paper we analyze the accumulated experimental data on $SrTiO_3$-based SOFC anodes in the framework of the existing point defect model of *n*-doped $SrTiO_3$. We also critically revised and extended our results on Sr-deficient niobium and yttrium doped $SrTiO_3$ which confirm the general predictions of the defect chemistry model.

## 2. Experimental

Samples of $Sr_{1-x/2}Nb_xTi_{1-x}O_3$ where $x = 0.01$, 0.05, 0.1, 0.17, 0.2, 0.3, 0.4 and 0.6 were prepared by a solid state reaction method from $SrCO_3$, $TiO_2$ and $Nb_2O_5$ precursors of 99.9% purity (Cerac). Several selected compositions of $Sr_{1-3x/2}Y_xTiO_3$ and $Sr_{1-3x/2-y/2}Y_xNb_yTi_{1-y}O_3$ were prepared in a similar fashion. Stoichiometric mixtures were calcined for 10 h in air at 1200°C and sintered for 5 h at 1380–1400°C in air or forming gas of 7% $H_2$/93% Ar. Samples of 94–98% apparent density were obtained by this process. Powder XRD analysis was obtained from a Bruker D8 X-ray diffractometer with monochromatic Cu $K_{\alpha 1}$ radiation. Selected samples were polished and chemically etched in $H_3PO_4$ and examined by SEM (Philips 515) equipped with EDX (Link Analytical). Cylindrical samples 15 mm long and 6 mm diameter were used for conductivity measurements. The air-sintered samples were annealed in forming gas at 850°C for 24 hours. The oxygen partial pressure during the dc four-point conductivity measurements at 800°C was fixed by a mixture of CO and $CO_2$ gases with a controlled ratio using 1159B-type MKS mass-flow controller. Selected samples sintered in forming gas were oxidized at 1250°C in air and their conductivity was measured as a function of $P_{O_2}$.

## 3. Results and Discussion

In this study the Nb-doped $SrTiO_3$ compounds were formulated assuming the Sr-vacancy compensation of donors. Thus we expected that ceramics sintered in air would be insulating and single-phase. Both SEM and XRD analysis confirmed that the $Sr_{1-x/2}Nb_xTi_{1-x}O_3$ compounds sintered in air remain single phase up to $x = 0.30$ (Fig. 1). This solubility limit is in good agreement with the data of Slater et al. [3]. who obtained nearly single phase $Sr_{1-x/2}Nb_xTi_{1-x}O_3$ with $x \leq 0.4$. For the $Sr_{1-3x/2}Y_xTiO_3$ system prepared at $P_{O_2} = 0.2$ atm, the solubility limit of yttrium was found to be around 4%, lower than $x = 0.08$ reported earlier by Hui [4]. At higher yttrium concentration, the $Y_2Ti_2O_7$ pyrochlore phase appears consistently. The Y and Nb co-doped samples (e.g., $Sr_{1-3x/2-y/2}Y_xNb_yTi_{1-y}O_3$) remain single phase up to $x = 0.04$ and $y = 0.2$ when sintered in air.

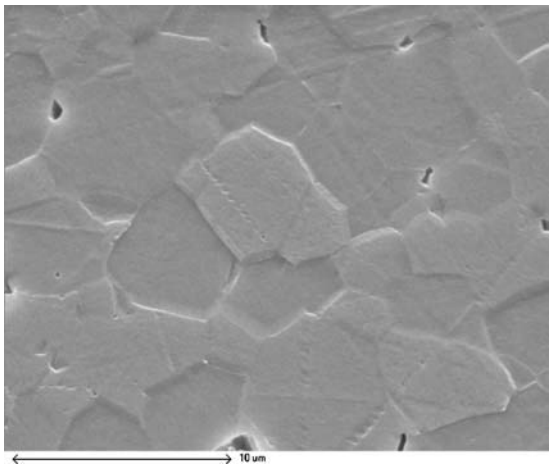


*Fig. 1.* SEM of single phase $Sr_{0.85}Ti_{0.7}Nb_{0.3}O_3$ sintered in air.

Consider what may occur when Sr-deficient $Sr_{1-3x/2}Y_xTiO_3$ or $Sr_{1-x/2}Nb_xTi_{1-x}O_3$ is subjected to low $P_{O_2}$ during sintering. According to the defect chemistry model, the donor compensation mechanism should shift from the *cation vacancy* to the *electronic* type. By analogy with Eq. (2), one would expect accommodation of Ti excess by precipitation of Ti-rich second phases according to the following transformation:

$$Sr_{1-3x/2}Y_xTiO_3 \Rightarrow Sr_{1-3x/2}Y_xTi_{1-x/2}O_3 + \frac{x}{2}TiO_{2(MDL/MP)}, \quad (3)$$

where $TiO_{2(MDL/MP)}$ are either $TiO_2$ Magneli double layers (MDL) embedded into the $SrTiO_3$ matrix [28] or precipitated $Ti_nO_{2n-1}$ Magneli phases (MP) [29]. Surprisingly, for $Sr_{1-x/2}Nb_xTi_{1-x}O_3$ sintered in forming gas, the XRD analysis did not detect any second phase up to $x \leq 0.20$. Since this was in disagreement with the usual model for donor-doped $SrTiO_3$ we performed a detailed SEM/EDX analysis of a sample with $x = 0.17$ and were able to detect a substantial amount of Ti- and Nb-rich second phases in this

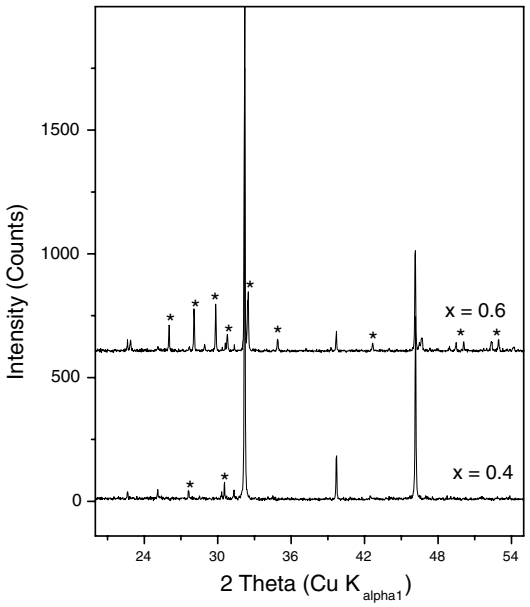


*Fig. 2.* XRD of $Sr_{1-x/2}Nb_xTi_{1-x}O_3$ with $x = 0.4$ and $x = 0.6$. The $Sr_3TiNb_4O_{15}$ phase is labelled with *.

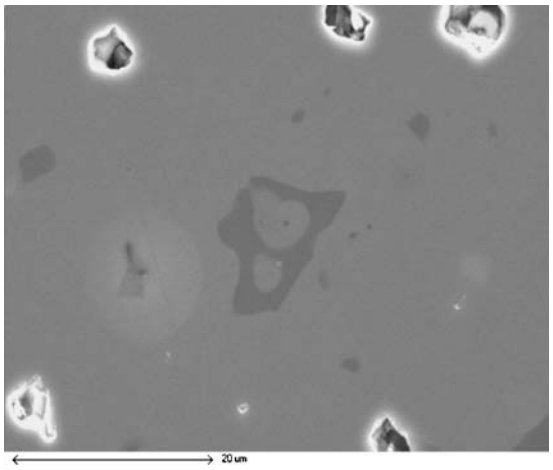


*Fig. 3.* SEM of $Sr_{0.915}Ti_{0.83}Nb_{0.17}O_3$ sintered in forming gas. The dark grey regions are Sr-deficient second phase.

sample (Fig. 3) as expected. Above $x = 0.20$, the $Sr_3TiNb_4O_{15}$ second phase appears in the XRD pattern (Fig. 2). Figure 4 shows another example of the multiphase compound obtained from the starting composition of $Sr_{0.84}Y_{0.04}Ti_{0.8}Nb_{0.2}O_3$ sintered in forming gas. The Ti/Nb-rich and Y+Ti-rich second phases develop in ceramics sintered at low $P_{O_2}$. The chemical composition of the matrix and second phases determined by the EDX analysis are listed in Table 1.

*Table 1.* EDX chemical analysis (wt%) of second phases in *n*-doped $SrTiO_3$.

| Compound/Element | Matrix | Ti-rich | Nb-rich | Ti+Y-rich |
|---|---|---|---|---|
| $Sr_{0.84}Y_{0.04}Ti_{0.8}Nb_{0.2}O_3$ | | | | |
| Sr | 54 | 25 | 37 | 0.42 |
| Y | 2 | 0 | 0 | 53.1 |
| Ti | 28 | 65 | 7.36 | 44.5 |
| Nb | 13.5 | 8.1 | 55 | 2.6 |
| $Sr_{0.915}Ti_{0.83}Nb_{0.17}O_3$ | | | | |
| Sr | 59 | 25 | 37.0 | |
| Ti | 29.3 | 65 | 7.0 | |
| Nb | 11.6 | 8.1 | 55.7 | |

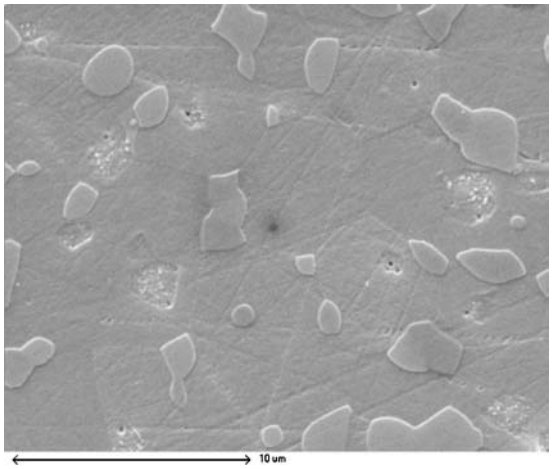


*Fig. 4.* SEM of chemically etched $Sr_{0.84}Y_{0.04}Ti_{0.8}Nb_{0.2}O_3$ sintered in forming gas. Precipitates of the Ti/Nb-rich and Ti+Y-rich second phases are seen as regions of raised relief.

The conductivity of as-sintered and oxidized samples was studied at $P_{O_2} = 10^{-20}$–$10^{-14}$ atm. Each $P_{O_2}$ data point in Fig. 5 was recorded after 72-hour equilibration at 800°C. However, due to the extremely slow kinetics of strontium vacancies at 800°C, the results in Fig. 5 by no means should be interpreted as a true *equilibrium* conductivity. According to Fig. 5, the samples sintered at 1400°C in $H_2/N_2$ show the highest $\sigma$ values. Measured at 800°C in low $P_{O_2}$, conductivities of 339 S/cm and 98 S/cm were achieved for $Sr_{0.9}Ti_{0.8}Nb_{0.2}O_3$ and $Sr_{0.88}Y_{0.08}TiO_3$ samples sintered in forming gas. The conductivity values of the samples sintered in reducing atmosphere are compared with the conductivity of the $Sr_{1-x}La_xTiO_3$ ceramics derived from Ref. [10]. The results shown in Fig. 6 suggest that Sr-deficient *n*-doped $SrTiO_3$

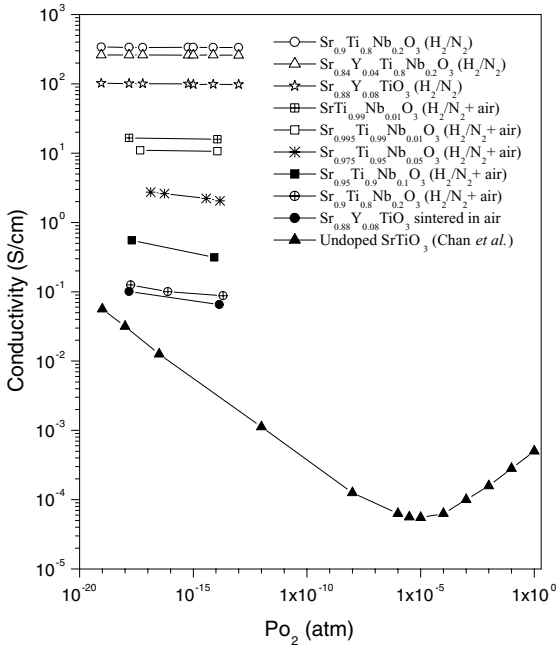


*Fig. 5*. Conductivity of Nb- and Y-doped $SrTiO_3$ compositions at 800°C and different $P_{O_2}$. The legend $H_2/N_2$ stands for samples sintered in forming gas. The legend $H_2/N_2$ + air stands for samples sintered in forming gas and oxidized at 1250°C in air. The data for undoped $SrTiO_3$ were taken from ref. [30].

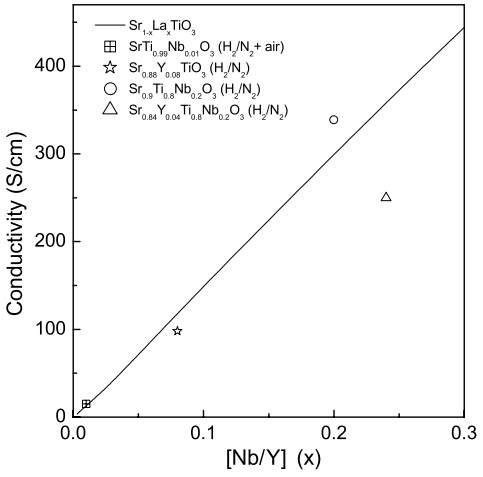


*Fig. 6*. Conductivity of La-, Nb- and Y-doped $SrTiO_3$ compositions at 800°C. The data for $Sr_{1-x}La_xTiO_3$ ceramics was derived from Ref. [10]. The legend $H_2/N_2$ stands for samples sintered in forming gas. The legend $H_2/N_2$ + air stands for samples sintered in forming gas and oxidized at 1250°C in air.

sintered in forming gas possess a high degree of electronic compensation. Moreover, the conductivity of Sr-deficient $Sr_{0.9}Ti_{0.8}Nb_{0.2}O_3$ sintered at low $P_{O_2}$ slightly exceeds the conductivity of electronically compensated $Sr_{0.8}La_{0.2}TiO_3$ from Ref. [10] which indicates that electron mobility of Nb-doped $SrTiO_3$ is higher than that of La-doped $SrTiO_3$.

When as-sintered samples were *oxidized in air* at 1250°C, and reduced at 850°C for 24 hours, the conductivity decreased by orders of magnitude compared to the initial "as-sintered" value. The largest drop in conductivity was observed for heavily doped samples. For example, the conductivity of $Sr_{0.9}Ti_{0.8}Nb_{0.2}O_3$ dropped from 339 S/cm to 0.12 S/cm after oxidation followed by low-temperature reduction. In contrast, the conductivity of lightly doped samples, such as $Sr_{0.995}Ti_{0.99}Nb_{0.01}O_3$, did not change significantly and remained at 9.8 S/cm level after oxidation/reduction anneal. Both "as-sintered" and oxidized/reduced samples showed a nearly $P_{O_2}$ independent conductivity in the $P_{O_2} = 10^{-20}$–$10^{-14}$ atm range (Fig. 5).

In general, our results support the defect chemistry model of donor-doped $SrTiO_3$ i.e., a Sr-deficient *n*-doped $SrTiO_3$ sintered at low $P_{O_2}$ transforms into a multiphase material with Ti-rich second phases. The conductivity of this multiphase composition would depend on the degree of electronic compensation of donors in the major phase, which in turn, depends on the oxygen activity during sintering. This explains the high values of electronic conductivity of our Sr-deficient *n*-doped $SrTiO_3$ samples sintered in forming gas (Fig. 5). Furthermore, since Y and Nb donors are now electronically compensated, the overall dependence of $\sigma$ on $P_{O_2}$ should be similar to that of the $Sr_{1-x}La_xTiO_3$ composition reported by Moos and Härdtl [17]. A characteristic feature of this behavior is a "plateau region" in the $\sigma$ *versus* $P_{O_2}$ dependence which is unambiguously observed in Fig. 5.

When samples sintered at low $P_{O_2}$ are subjected to high $P_{O_2}$ during oxidation at 1250°C, Eq. (2) comes into effect. Owing to the very slow diffusion of strontium vacancies, the reaction will require substantial temperature or time to reach equilibrium. This means that part of the donor dopants will remain compensated by electrons at least in the grain bulk. It may be argued that the equilibrium will never be achieved at SOFC operating temperatures. That is why the conductivity of oxidized samples does not recover to its original value after in situ reduction at 850°C. Furthermore, one

may expect that the kinetics of reactions 1 and 2 will be slower in dense polycrystalline samples since the formation of the second phases will induce significant strain in the matrix grains and eventually will be elastically arrested. This explains the different behavior of $\sigma$ *versus* $P_{O_2}$ dependence reported by Slater et al. for dense and porous samples [3]. Another consequence of this process would be development of microcracks in dense samples during oxidation-reduction cycling as observed in our study and also reported by Marina et al. [5].

As mentioned in the introduction, the standard SOFC processing route includes co-sintering of the NiO-YSZ anode and electrolyte layers followed by firing of the screen printed cathode layer. The final step involves in-situ reduction of the anode at the SOFC operating conditions. The normal sintering temperatures for the SOFC stack range from 1200 to 1400°C. Figure 5 shows conductivity of $Sr_{0.88}Y_{0.08}TiO_3$ sample sintered in air at 1380°C and *in situ* annealed in reducing atmosphere at 850°C. The conductivity of this sample remained at 0.1 S/cm after 1 week of anneal compared to 98 S/cm and 1000 S/cm for the same sample sintered at low $P_{O_2}$ and for Ni-YSZ anode, respectively.

In this paper, we focused mainly on electronic conductivity of the Sr-deficient *n*-type $SrTiO_3$. However, high electronic and high ionic conductivities as well as high catalytic activity are required for efficient SOFC anode performance. The oxygen conductivity of *n*-type $SrTiO_3$ is orders of magnitude lower than the electronic one. However, even at conductivities of $10^{-4}$ S/cm, some ionic diffusion is possible. The SOFC anode would still require a mixed ceramic, such as YSZ+*n*-type $SrTiO_3$ to achieve transport of the two species but the presence of some mixed conduction allows the reaction to occur over a wider surface than just at the triple phase boundary line as occurs in the Ni-YSZ. Another problem is catalytic activity of the SOFC anode. Unlike Ni, which is a good catalyst in the Ni-YSZ based anodes, the *n*-type $SrTiO_3$ is not a catalyst. That is why several research groups have been adding $CeO_2$ or other catalysts to promote the anodic reaction [5, 6]. Certainly, much more work must be done to realize a competitive $SrTiO_3$-based SOFC anode.

## 4. Conclusions

We analyzed yttrium and niobium-doped $SrTiO_3$ where charge compensation was extrinsically realized by strontium vacancies. It was found that these compounds transform from a single phase when sintered in air to multi-phase when sintered in a reducing atmosphere. The EDX analysis revealed that the second phases are strontium deficient, which is in excellent agreement with a defect chemistry model of donor-doped $SrTiO_3$. From a practical viewpoint, the realization of a $SrTiO_3$-based SOFC anode seems to be much more challenging than originally expected. Despite significant progress, the conductivity of the dense *n*-doped $SrTiO_3$ sintered in air at 1200–1400°C and measured at typical SOFC anode conditions is still orders of magnitude lower than that of the conventional Ni-YSZ cermet anode. However, the phase stability of *n*-doped $SrTiO_3$ is maintained at the SOFC operation conditions due to the very slow kinetics of cations at 800°C.

## Acknowledgments

The authors acknowledge financial support of the Natural Sciences and Engineering Research Council of Canada, National Research Council and Versa Power Systems Ltd. (formerly Global Thermoelectric). Part of this study was performed through Special Coordination Funds for Promoting Science and Technology from the Ministry of Education, Culture, Sports, Science and Technology of the Japanese Government.

## References

1. S.J. Visco, C.P. Jacobson, I.Villareal, A. Leming, Y. Matus, and L.C. deJonghe, *Electrochem. Soc. Proc.*, **2003-07**, 1040 (2003).
2. G. Pudmich, W. Jugen, and F. Tiez, in *6-th Int. Solid Oxide Fuel Cell Symp., Electrochemical Society Proceedings*, edited by S.C Singhal and M. Dokiya (1999) vol. 99–19, p. 577.
3. P.R. Slater, D.P. Fagg, and J.T.S. Irvine, *J. Mater. Chem.*, **7**, 2495 (1997).
4. S. Hui and A. Petric, *J. Electrochem. Soc.*, **149**, J1 (2002).
5. O.A. Marina, N.L. Canfield, and J.W. Stevenson, *Solid State Ionics*, **149**, 21 (2002).
6. S. Koutcheiko, Y. Yoo, and A. Petric, in *Proc. 5th European Solid Oxide Fuel Cell Forum, Lucerne (CH)* (2002) vol. 2, p. 655.
7. S. Hui, Ph.D. Thesis, Evaluation of the *n*-doped $SrTiO_3$ for solid oxide fuel cell anode. McMaster University, Hamilton, Canada, 2000.
8. H.P.R. Frederikse, W.R. Hosler, W.R. Thurber, J. Babiskin, and P.G. Siebermann, *Phys. Rev.*, **158**, 775 (1967).
9. D.M. Eagles, in *Physics of Disordered Materials*, edited by D. Adler (Plenum, New York, 1985), p. 357.
10. R.Moos, S. Schöllhammer, and K.H. Härdtl, *Appl. Phys. A*, **65**, 291 (1997).

11. P. Calvani, M.Capizzi, F. Donato, S. Lupi, P. Maselli, and D. Peschiaroli, *Phys. Rev. B.*, **47**, 8917 (1993).
12. R. Moos, A. Gnudi, and K.H. Härdtl, *J. Appl. Phys.*, **78**, 5042 (1995).
13. C. Lee, J. Destry, and J.L. Brebner, *Phys. Rev. B.*, **11**, 2299 (1975).
14. D.A. Crandles, B. Nicholas, C. Dreher, C.C. Homes, A.W. McConnell, B.P. Clayman, W.H. Gong, and J.E. Greedan, *Phys. Rev. B.*, **59**, 12842 (1999).
15. F. Gervais, J.-L. Servoin, A. Baratoff, J.G. Bednorz, and G. Binnig, *Phys. Rev. B.*, **47**, 8187 (1993).
16. A.M.J.H. Seuter, *Philips Res. Repts.*, **3**(Suppl) 1 (1974).
17. R. Moos and K.H. Härdtl, *J. Am. Ceram. Soc.*, **80**, 2549 (1997).
18. D.M. Smyth, *J.Electroceram.*, **9**, 179 (2002).
19. R. Meyer and R. Waser, *Sensors and Actuators B*, **101**, 335 (2004).
20. M.J. Akhtar, Z-U-N Akhtar, R.A. Jackson, and C.R.A. Catlow, *J. Am. Ceram. Soc.*, **78**, 421 (1995).
21. R. Meyer, R. Waser, J. Helmbold, and G. Borchardt, *J. Electroceramics.*, **9**, 103 (2002).
22. J. Daniels and K.H. Härdtl, *Philips Res. Repts.*, **31**, 489 (1976).
23. U. Balachandran and N.G. Eror, *J. Electrochem. Soc.*, **129**, 1021 (1982).
24. R. Moos, T. Bischoff, W. Menesklou, and K.H. Härdtl, *J. Mater. Sci.*, **32**, 4247 (1997).
25. S.N.Ruddlesden and P.Popper, *Acta Crystall.*, **11**, 54 (1958).
26. P.D. Battle, J.E. Bennett, J. Sloan, R.J.D. Tilley, and J.F. Vente, *J. Solid State Chem.*, **149**, 360 (2000).
27. W. Menesklou, H-J. Schreiner, K.H. Härdtl, and E. Ivers-Tiffée, *Sensors and Actuators B*, **59**, 184 (1999).
28. T. Suzuki, Y. Nishi, and M Fujimoto, *Philos. Mag. A*, **80**, 621 (2000).
29. M. Fujimoto and M. Watanabe, *J. Mater. Sci.*, **20**, 3683 (1985).
30. N.-H. Chan, R.K. Sharma, and D.M. Smyth, *J. Electrochem. Soc.*, **128**, 1762 (1981).